Capacitive-Coupling-Enhanced Switching Gain in an Electron Y-Branch Switch

S. Reitzenstein, L. Worschech, P. Hartmann, M. Kamp, and A. Forchel

Technische Physik, Universität Würzburg, Am Hubland, D-97074 Würzburg, Germany

(Received 15 July 2002; published 7 November 2002)

We have fabricated electron Y-branch switches (YBS) on modulation doped GaAs/AlGaAs heterostructures. The Y branch consists of a one-dimensional source, which is split along the branching section into two one-dimensional drains. In addition to source drain voltages, external electric fields can be applied via gates along the branches.In the nonlinear transport regime sweeps of the side-gate voltages lead to a voltage difference between the drain reservoirs with gain. This switching gain increases superlinearly with the bias voltage applied between the source and the drains of the YBS. We explain the bias voltage enhanced switching by a capacitive coupling of the branches.

DOI: 10.1103/PhysRevLett.89.226804 PACS numbers: 73.50.–h, 73.63.–b

Switching of electrons in nanoelectronic junctions is of interest both from a basic physics point of view as well as for future applications [1–5]. Gate induced switching depends sensitively on the capacitance, which relates changes in charge density of the switch to the voltage sweep of the gate [6,7]. For switching important structural parameters are, for example, the separation length between the gate and the conducting channel or the length of the gate. Nowadays modern semiconductor fabrication technologies are successfully used to realize switching devices with gate lengths in the order of 10–100 nm [8]. However, with decreasing gate length the electric field built up by voltage differences between the source and the drain increases, which in turn influences more and more the switching field.

A device of special interest is an electron Y-branch switch (YBS), as it is based on the smallest transport zone of a three terminal junction [9]. In a YBS a one-dimensional source is split into two one-dimensional drains. In the linear transport regime with small bias voltages applied between the source and the drains pronounced switching has been demonstrated [4,10]. Switching is then due to a side-gate controlled lateral switching field, which directs electrons from the stem into either of the branches [9,11,12]. However, when the switching length of the YBS is in the order of the gate distance, sufficient large voltage differences between the source and the drains or between the branches themselves lead to intrinsic electric fields which modify the effective switching field. Using a simple way of argumentation the electron path in a YBS along which a larger voltage bias exists is expected to carry a larger current. On the other side, it is well known that, with increasing current scattering leads to a randomization of electron momentum [13,14]. It has also been stated that intrinsic gating effects may play an important role when we leave equilibrium [15]. Recently, Wesström predicted a self-gating mechanism due to a capacitive coupling of the branches in a YBS, dominating the switching field [1]. Despite the fundamental issues for switching properties of gate controlled, ultrashort junctions, experimental studies of the capacitive coupling between different channels and their influence in the switching characteristics have to our knowledge not been performed up to now.

Here we present results on a capacitive coupling enhanced switching effect of an electron Y-branch switch in the nonlinear transport regime. It is found that voltage sweeps applied to the side-gates of the YBS lead to pronounced voltage differences between the branches resulting in gain. The switching gain increases superlinearly with the bias voltage between the source and the drains. The enhanced switching is interpreted in terms of a capacitive coupling of the branches. Our results provide new insights in the switching mechanisms of nanoelectronic junctions.

The samples were fabricated by electron beam lithography and wet etching of modulation doped GaAs/AlGaAs heterostructures with a two-dimensional electron gas (2DEG) located 80 nm below the surface. From Hall measurements it was determined that the mean free path of the electrons exceeds 10 μm for the unprocessed wafer at $T = 4.2$ K in the dark. A scanning electron microscope graph of a YBS similar to that investigated is shown in the center part of Fig. 1. The stem splits along the branching section with a length of 70 nm into a left and a right branch. Trenches 180 nm wide and 90 nm deep define the YBS as well as two lateral side-gates further used to control the switching of electrons into either of the branches. The side-gate voltages define the working-point of the Y branch, which was adjusted to achieve single-mode operation in the linear transport regime [10].

Switching characteristics of the YBS were analyzed using the setup schematically sketched in Fig. 1. The bias voltage V_{bias} was applied between the source and the drains in series with resistors $R_b = 10$ MΩ. High impedance voltmeters were used to detect the voltages V_{bl} and V_{br} at the reservoirs of the left branch and the right branch, respectively. The stem reservoir was connected to ground via a resistor $R_s = 120$ kΩ. All

 © 2002 The American Physical Society

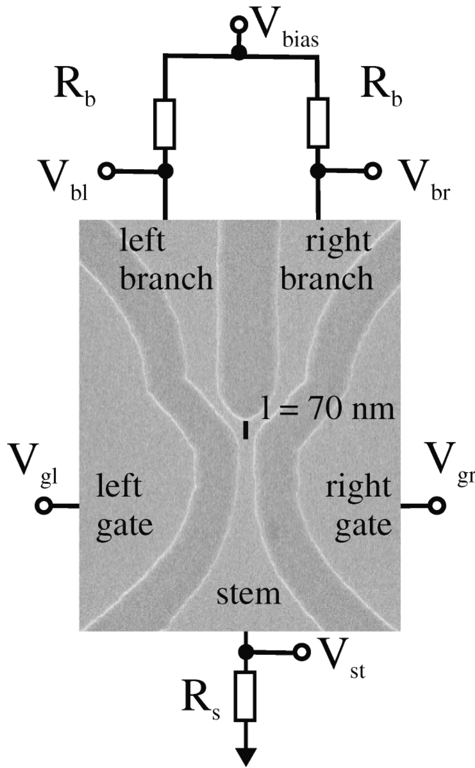

FIG. 1. Scanning electron microscope (SEM) image of a YBS with a length $l = 70$ nm of the branching section and a schematic view of the measurement configuration. Separated by etched trenches from the nanojunction the left and the right side-gate allow one to direct electrons into either of the branches. The bias voltage V_{bias} was applied via two resistors ($R_b = 10$ MΩ) to the left and the right branch of the YBS, with the stem coupled to ground via $R_s = 120$ kΩ. High impedance voltmeters were used to measure the voltage V_{st} at the stem as well as the voltages V_{bl} and V_{br} at the left and the right branch, respectively. All voltages are related to ground.

measurements were performed at 4.2 K by immersing the samples in liquid helium.

In order to investigate switching of electrons in the YBS we have detected the voltage differences $V_{bl} - V_{br}$ for voltage sweeps at the side-gates in push-pull fashion, i.e., $\delta V_{gl} = -\delta V_{gr}$, with voltages V_{gl} and V_{gr} applied to the left and the right side-gate, respectively. In Fig. 2(a) V_{bl} and V_{br} are plotted versus $\Delta V_g = V_{gl} - V_{gr} + V_{g,\text{asym}}$ for different bias voltages. For the sake of clarity we have shifted the gate voltage difference by $V_{g,\text{asym}} = -0.38$ V, which we relate to an unintended asymmetry of the YBS. For $\Delta V_g < -0.2$ V and $V_{\text{bias}} = 1.75$ V electrons are directed effectively into the right branch and the current into the left branch vanishes. Thus the voltage $V_{br} = V_{\text{bias}} - I_r R_b$. In contrast, the voltage at the left branch $V_{bl} = V_{\text{bias}} - I_l R_b$ tends towards V_{bias} as I_l is negligibly small. With increasing ΔV_g the current through the right branch I_r decreases and I_l simultaneously increases. For $\Delta V_g > 0.2$ V the right branch is pinched off ($V_{br} \approx V_{\text{bias}}$). As one can see in Fig. 2(a) the described switching behavior is in fact similar for $V_{\text{bias}} = 1.00$ and 0.50 V. However, the voltages V_{bl} and V_{br} do not reach the applied bias voltage for $|\Delta V_g| < 0.2$ V, indicating that for smaller V_{bias} the switching of electrons is less efficient.

We have been able to observe voltage gain for the present YBS. As depicted in Fig. 2(b), for $|\Delta V_g| < 0.1$ V and $V_{\text{bias}} = 1.75$ V changes in the voltage difference $V_{bl} - V_{br}$ exceed by far the gate voltage variation. In order to demonstrate that the switching efficiency of the YBS depends on the applied bias voltage we have plotted in the inset of Fig. 2(b) the minimum voltage sweep $V_{g,\min}$ requested for switching ΔV_b from $0.5V_{\text{bias}}$ to $-0.5V_{\text{bias}}$ versus bias voltages ranging from $V_{\text{bias}} = 0.1$ to 1.75 V. $V_{g,\min}$ decreases with increasing V_{bias} reflecting the enhanced switching properties for higher bias voltages; e.g., $V_{g,\min} = 65$ mV for $V_{\text{bias}} = 1.75$ V, whereas $V_{g,\min} = 225$ mV is required in the case of $V_{\text{bias}} = 0.5$ V. Thus, the switching is demonstrated to depend sensitively on the bias voltage V_{bias}.

In order to describe the observed switching we introduce two switching parameters γ_l and γ_r. Using these parameters the currents I_l and I_r through the left and the right branch can then be described by the voltage differences between the left branch and the stem and the right branch and the stem:

$$I_l = \tfrac{1}{2}G(1 + \gamma_l)(V_{bl} - V_{st}) \quad \text{and}$$
$$I_r = \tfrac{1}{2}G(1 - \gamma_r)(V_{br} - V_{st}), \tag{1}$$

with G a constant, which corresponds to the maximum conductance of the YBS for a given working-point. From the observed switching behavior it is clear that the

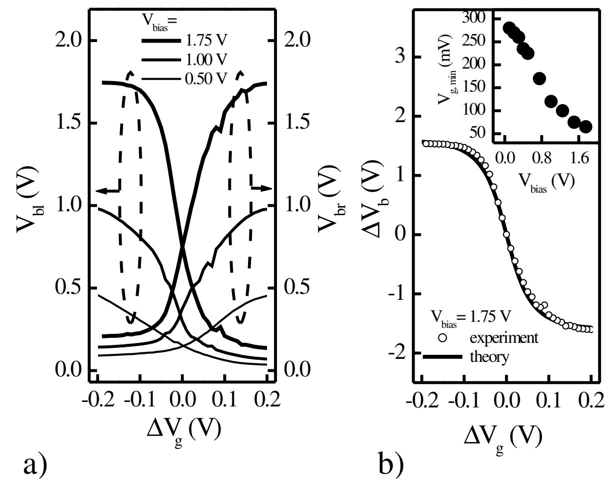

FIG. 2. (a) Voltages $V_{bl,r}$ detected at the left and the right branch reservoir vs the voltage difference $\Delta V_g = V_{gl} - V_{gr} + V_{g,\text{asym}}$ varied in push-pull fashion, i.e., $\delta V_{gl} = -\delta V_{gr}$. (b) Voltage difference $\Delta V_b = V_{bl} - V_{br}$ at the branches versus ΔV_g and the gate voltage $\Delta V_{g,\min}$ needed to switch from $\Delta V_b = 0.5V_{\text{bias}}$ to $\Delta V_b = -0.5V_{\text{bias}}$ as a function of V_{bias} (inset). The calculated curve corresponds to $\eta_g/V_s = 10.0$ V^{-1}, $\eta_b/V_s = -0.36$ V^{-1}, $G = 1.16 \times 10^{-6}$ Ω^{-1}, and $V_{wp} = 0.10$ V.

switching field increases with the applied bias voltage and thus γ_l and γ_r are functions not only of the gate voltage difference ΔV_g, but also of the voltage difference between the branches ΔV_b. Very good fitting to the experimental data was possible using the following short analytic expressions for the switching parameters:

$$\gamma_l = \tanh\left\{\frac{\eta_g(\Delta V_g - V_{wp}) + \eta_b \Delta V_b}{V_s}\right\},$$
$$\gamma_r = \tanh\left\{\frac{\eta_g(\Delta V_g + V_{wp}) + \eta_b \Delta V_b}{V_s}\right\}, \tag{2}$$

with η_g and η_b referred to as the gate efficiencies of the side-gate and of the branches, respectively. The switching voltage V_s is a measure of how large a change in the effective switching voltage V_s is required to affect γ_l and γ_r. It is noteworthy that γ_l and γ_r differ only by a constant shift $2V_{wp}$ of the side-gate voltage difference. V_{wp} is the working-point voltage and considers that the crossing-point $V_{bl} = V_{br}$ can be tuned by $V_{wp} = V_{gl} + V_{gr}$ when the gate voltages are swept in push-pull fashion. For example, with increasing V_{wp} the crossing-point is shifted towards smaller values of V_b. Taking into account that the voltage at the stem can be expressed by $V_{st} = (I_l + I_r)R_s$ with $I_{l,r} = (V_{\mathrm{bias}} - V_{bl,r})/R_B$, Eqs. (1) can be rewritten in the form

$$(V_{\mathrm{bias}} - V_{bl})/R_b = G\frac{1+\gamma_l}{2} \times \left\{V_{bl} - (2V_{\mathrm{bias}} - V_{bl} - V_{br})\frac{R_s}{R_b}\right\}, \tag{3a}$$

$$(V_{\mathrm{bias}} - V_{br})/R_b = G\frac{1-\gamma_r}{2} \times \left\{V_{br} - (2V_{\mathrm{bias}} - V_{bl} - V_{br})\frac{R_s}{R_b}\right\}. \tag{3b}$$

We have solved these coupled equations iteratively for varying fitting parameters η_g/V_s, η_b/V_s, and V_{wp}. In Fig. 2(b) a calculated ΔV_b versus ΔV_g characteristic is shown for $V_{\mathrm{bias}} = 1.75$ V with $\eta_g/V_s = 10.0\ \mathrm{V}^{-1}$, $\eta_b/V_s = -0.36\ \mathrm{V}^{-1}$, $G = 1.16 \times 10^{-6}\ \Omega^{-1}$, and $V_{wp} = 0.10$ V. It can be seen that the calculated $\Delta V_b(\Delta V_g)$ trace fits very well to the experimentally observed curve. This result indicates that the voltage differences between the branches influence the effective switching voltage.

In order to estimate the bias voltage induced enhanced switching we have determined the differential voltage gain $g = d(\Delta V_b)/d(\Delta V_g)$. In Fig. 3 the dependence of g on ΔV_g is shown. $|g|$ increases with decreasing $|\Delta V_{\mathrm{gate}}|$ leading to a pronounced maximum at $\Delta V_g = 0$. For the present device we found a maximum gain of $g_{\max} = -26.3$. In addition to the experimental data the curves calculated from Eq. (3) with subsequent numerical derivation of ΔV_b versus ΔV_g for different gating efficiences $\eta_b/V_s = 0, -0.25, -0.36$, and $-0.45\ \mathrm{V}^{-1}$, and constants $\eta_g/V_s = 10.0\ \mathrm{V}^{-1}$, $G = 1.16 \times 10^{-6}\ \Omega^{-1}$, as well as $V_{wp} = 0.10$ V are depicted in Fig. 3. According to our model for $\eta_b/V_s = 0$ a maximum gain of -13.7 is expected. However, the experimentally observed intrinsic gating efficiency per switching voltage of $\eta_b/V_s = -0.36\ \mathrm{V}^{-1}$ leads to a doubling of the maximum switching gain for $V_{\mathrm{bias}} = 1.75$ V.

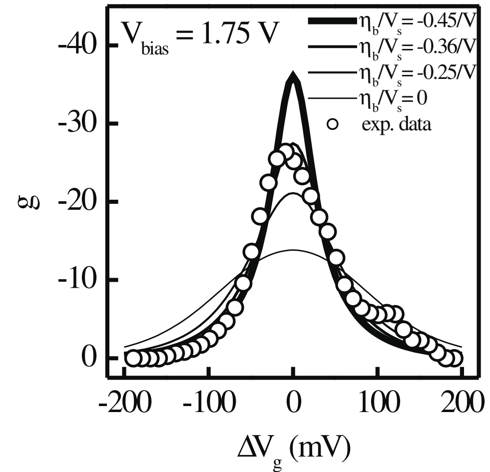

FIG. 3. Differential voltage gain g as a function of the gate voltage difference ΔV_g. The curves were calculated for gating efficiencies between $\eta_b/V_s = 0$ (no bias voltage induced gating) and $\eta_b/V_s = -0.45\ \mathrm{V}^{-1}$. The peak value of $|g|$ increases with increasing η_b/V_s, whereas the linewidth decreases.

To clarify the role of the intrinsic switching field on the YBS gain characteristic we have experimentally analyzed the maximum gain for different bias voltages and compared it to the calculated values extracted from Eqs. (3). In Fig. 4 these values are plotted versus V_{bias}. For bias voltages up to 0.5 V $g_{\max}$ increases almost linearly with V_{bias} reflecting a linear response of the gain to side-gate induced voltage changes. Here the side-gate controlled switching dominates. With increasing $V_{\mathrm{bias}} > 0.5$ V $g_{\max}$ increases superlinearly indicating that voltage differences between the branches have a significant influence on the effective switching field.

For a better discussion of the superlinear $g_{\max}(V_{\mathrm{bias}})$ characteristic it is useful to compare our results with the self-gating mechanism proposed by Wesström [1]. Wesström modified the model of Palm and Thylén [16] by taking into account a switching field, which depends on the potential difference between the branches. In fact, formal similar expressions to Eqs. (2) can be derived using the model suggested in Ref. [1] with $V_{wp} = 0$. Self-gating was introduced by a perturbation approach of a Landauer-Büttiker formula for a three terminal device adding a self-gating induced switching voltage to the side-gate induced switching voltage. From electron waveguide analogies a positive sign for the self-gating

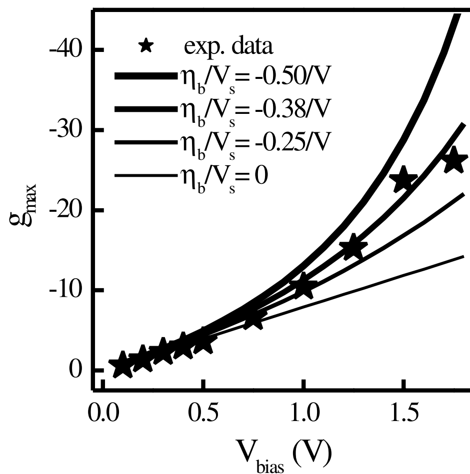

FIG. 4. Maximal differential voltage gain g_{max} as a function of the bias voltage V_{bias}. The data extracted from the experiment (★) is plotted together with curves calculated for different gating efficiencies η_b/V_s. For $\eta_b/V_s = 0$ (no bias induced gating) g_{max} is increasing linearly with V_{bias}. However, a nonlinear behavior was found for finite self-gating efficiencies ($\eta_b/V_s < 0$) in agreement with the experimental data.

efficiency was predicted, which would lead to a suppression of voltage gain for the present bias regime. Our observations show that the branches have a gate functionality similar to the side-gates; e.g., a more positive voltage at one branch relative to the other branch increases the conductance of the latter. This can be explained in terms of a capacitive coupling between the left and the right branch. The bias voltage enhanced switching gain is described by a negative sign of η_b. Another interesting effect of this branch coupling is that the noise features in the voltages V_{br} and V_{bl} are found to occur phase shifted; e.g., a close inspection of the V_{br} and V_{bl} traces in Fig. 2(a) shows that a slight increase in V_{bl} at $\Delta V_g = 0.09$ V is correlated with a dip in V_{br}. Thus a YBS in the present bias regime represents an interesting device for studies of noise signals [17].

The authors gratefully acknowledge financial support by the European Commission through the Information Society Technologies (IST) Programme Project NEAR and the state of Bavaria. Expert technological assistance by M. Emmerling and S. Reuss is gratefully acknowledged.

[1] J.-O. J. Wesström, Phys. Rev. Lett. **82**, 2564 (1999).
[2] C. Papadopoulos, A. Rakitin, J. Li, A. S. Vedeneev, and J. M. Xu, Phys. Rev. Lett. **85**, 3476 (2000).
[3] A. N. Andriotis, M. Menon, D. Srivastava, and L. Chernozatonskii, Phys. Rev. Lett. **87**, 066802 (2001).
[4] P. Omling, P. Ramvall, T. Palm, and L. Thylén, in *Proceedings of the 22nd International Conference on the Physics of Semiconductors* (World Scientific Publishing, River Edge, NJ, 1994), p. 1649.
[5] K. Hieke and M. Ulfward, Phys. Rev. B **62**, 16 727 (2000).
[6] D. K. de Vries, P. Stelmaszyk, and A. D. Wieck, J. Appl. Phys. **79**, 8087 (1996).
[7] Ya. M. Blanter, F. W. J. Hekking, and M. Büttiker, Phys. Rev. Lett. **81**, 1925 (1998).
[8] "International Technology Roadmap for Semiconductors" (Semiconductor Industry Association, San Jose, CA, 2001) (http://public.itrs.net/).
[9] T. Palm and L. Thylén, Appl. Phys. Lett. **60**, 237 (1992).
[10] L. Worschech, B. Weidner, S. Reitzenstein, and A. Forchel, Appl. Phys. Lett. **78**, 3325 (2001).
[11] T. Palm, J. Appl. Phys. **74**, 3551 (1993).
[12] T. Palm, L. Thylén, O. Nilsson, and C. Svensson, J. Appl. Phys. **74**, 687 (1993).
[13] U. Sivan, M. Heiblum, and C. P. Umbach, Phys. Rev. Lett. **63**, 992 (1989).
[14] Rita Gupta, N. Balkan, and B. K. Ridley, Phys. Rev. B **46**, 7745 (1992).
[15] R. Landauer, IBM J. Res. Dev. **32**, 306 (1988).
[16] T. Palm and L. Thylén, J. Appl. Phys. **79**, 8076 (1996).
[17] C. Dekker *et al.*, Phys. Rev. Lett. **66**, 2148 (1991).